Received May 26, 2019, accepted June 18, 2019, date of publication June 27, 2019, date of current version July 15, 2019.

Digital Object Identifier 10.1109/ACCESS.2019.2925431

Evaluation of Machine Learnable Bandwidth Allocation Strategy for User Cooperative Traffic Forwarding

LIN SHAN[1], (Member, IEEE), OU ZHAO[1], KATSUHIRO TEMMA[1], (Member, IEEE), KIYOHIKO HATTORI[2], FUMIHIDE KOJIMA[1], (Member, IEEE), AND FUMIYUKI ADACHI[3], (Fellow, IEEE)

[1]Wireless Systems Laboratory, National Institute of Information and Communications Technology, Tokyo 239-0847, Japan
[2]Saitama Institute of Technology, Fukaya 369-0203, Japan
[3]Research Wireless Signal Processing Research Group, Research Organization of Electrical Communication (ROEC), Tohoku University, Sendai 980-8577, Japan

Corresponding author: Lin Shan (shanlin@nict.go.jp)

This work was supported in part by the SECOM Science and Technology Foundation, Japan.

ABSTRACT In recent years, user cooperative traffic forwarding is a popular study topic and broadly seen as one of the important promising technologies to improve energy efficiency (EE) of the battery-driven mobile terminal (MT). However, the battery-driven devices always suffer from a problem of limited working time due to battery life. In this paper, we propose a simply machine learnable bandwidth allocation strategy for user cooperation-aided wireless communication systems and evaluate the power consumption of the systems via both theoretical and experimental approaches. By using the proposed bandwidth allocation strategy, we first derive the mathematical expressions to evaluate the transmission power of the MTs for non-cooperative and cooperative scenarios by a generalized channel model. In this generalized model, the spatially correlated shadowing and frequency selective fading are considered as channel effects, and this generalized model is mathematically analyzed for the consumed power via the proposed scenarios with the long-term evolution (LTE) power model for smartphones. In the final stage, we evaluate the results by our smartphone test-bed. The results obtained in this paper show that the benefits of the user cooperation-aided traffic forwarding are significant. Unfortunately, according to the numerical analysis, because there are some physical constraints for MTs, such as maximal transmit power, we cannot drastically obtain the benefits in real application cases. Some interesting points, such as how to use a machine learning approach to reduce the system complexity and thus improve transmission performances, are also discussed in this paper.

INDEX TERMS User cooperation, machine learning, device-to-device communication, frequency selective fading, power consumption, energy efficiency, ergodic capacity.

I. INTRODUCTION

Because of the rapid and explosive development of wireless applications [1], recently the mobile terminals (MTs) are very popular and important to modern people for various kinds of network communication demands in cellular systems, for example, high-definition video streaming, online gaming for multiple users, and instant text messaging, etc. As the MT applications are growing dramatically, the traffic loading of network and the power consumption of each MT become very important issues for modern mobile networks. In order to lower this kind of transmission loading and improve the performance of power saving for each MT in an effective and efficient way, forwarding transmission by utilizing cooperative wireless methods among MTs, which is also called user cooperation or cooperative communications, is widely considered and investigated as a promising approach to solve these issues [2], [3]. The cooperative traffic forwarding can achieve higher spectrum utility and energy efficiency (EE) [4] by using the device-to-device (D2D) transmission methods. In current wireless technology standards like Long Term Evolution (LTE) direct and Wi-Fi

The associate editor coordinating the review of this manuscript and approving it for publication was Guan Gui.

direct [5], D2D communications has been realizable in practice cases [6], and have motivated industry standardization efforts as well as a lot of academic researches [7].

In order to implement user cooperative traffic forwarding, a series of processes, for example, link sensing and configuration, especially, choice of a proper proxy, which is also called aggregator or head-MT [8], are needed. For this topic, many studies about how to select a proper proxy in wireless sensor networks, for example, low energy adaptive clustering hierarchy, well known as the LEACH technology [9] and so on [10], can be found in the literatures. In recent years, although several proxy selection methods have already been proposed and this topic have been widely researched, the existing transmission schemes are less related to the issue about how to use spectrum resource effectively. Besides, these schemes cannot be implemented directly on cellular systems because they are not designed for being applied on higher data rate transmission applications, and cannot well take the advantage of the channel state due to that base stations (BSs) are hard to consistently control the nodes. Henceforth, user cooperative communication technique adopted in cellular systems has been very attractive to academic and industrial groups.

In recent years, lots of studies, for example, [11]–[14], have investigated the issue of consumed power by user cooperation in cellular systems. In literature [11], the authors studied the terminal cooperation based traffic downloading for content distributing of MTs. From the results in [11], it can be known that cooperative communication can considerably increase the system EE. Because in download case, BS mainly consumed the energy rather than MTs, the results and the proposed method in [11] are useful for network operators. In [12], in order to increase the EE of two-MT used cooperative cognitive wireless networks with network coding, two novel schemes about power allocation are proposed. Further, the authors in [13] mathematically analyzed the tradeoff between the throughput and consumed energy in cooperative cognitive radio network. In [14], minimization of energy consumption issue with the use of cooperative communication for multi-hop networks have been investigated. Although the authors of the papers mentioned above considered the forwarding traffic in their papers, they all adopted a simple flat fading model in their simulations as attenuation environment for all the MTs.

It is well known that, because single carrier used communication has low peak-to-average power ratio and thus each MT can get great benefit in terms of the reduced cost on the power amplifier and the transmit power efficiency, such kind of communication technique has been adopted and applied as an appropriate access scheme in uplink cellular systems. By using the user cooperation aided forwarding approach, when compared with non-cooperative schemes and in order to deliver the total communication demands which are collected from other MTs, the proxy tends to be allocated more bandwidth or spectrum resource and may undergo frequency selective fading. As a result, proxy's transmission performance is worse than we expected. In our survey, there is no previous work discussing about this issue, which is very important and may affect the system performance significantly.

In addition, for traffic forwarding issue, basically BS needs to know uplink CSI of all MTs so that it can deal with the tasks of proxy selection and results informing [15]. Due to the delay in the network, it is difficult to deal with the cases which are sensitive to mobile transmission. Fortunately, with a growing development in artificial intelligence (AI), machine learning (ML) technique, which is a subset of AI, is going to become a good technology to provide alternative solutions to various issues in many wireless communication systems [16]–[21]. For example, in [18], the modulation recognition problem for cognitive radio (CR) communications is solved by ML based method. Similarly, precoding problem in millimeter-wave used multiple-input-multiple-output (MIMO) systems with the use of massive antenna deployment can be also solved in [19]. Therefore, introducing machine learning methods is a good choice for the considered traffic forwarding.

According to the discussion above, in this study, we propose a simply machine learnable bandwidth allocation strategy for user cooperative traffic forwarding, and evaluate the power consumption of the systems by both theoretical and experimental methods. In order to fit the present study to the real transmission environment closely, in this study, we employ a generalized channel attenuation model in which frequency selective fading channel and effect of spatially correlated shadowing are considered. Besides, in order to analyze the user cooperation aided forwarding scenario, we also introduce a recent LTE smartphone based power consumption model, which can make the results more convincing. Finally, a smartphone test-bed based experiment is also conducted to conclude our study.

In summary, we list the contributions of this study as follows.

- In this paper, we investigate the issue of user cooperative traffic loading with a generalized channel model. In the past, this issue is usually studied with some relatively simple channel assumptions, which are not suitable and are difficult to be applied on real wireless systems. Therefore, to enhance the contribution of our work, we adopt a generalized model including shadowing and fading effects to investigate the user cooperative traffic loading issue.
- To validate our proposed scenario, we evaluate the issue by both theoretical and experimental ways. Firstly we derive the related mathematical expressions and calculate the numerical results. By setting basics transmission parameters like transmission power, bandwidth, and number of MTs etc., the capacity over frequency selective channels with the use of proposed cooperative transmission scenario can be simply calculated without huge computational cost in simulation. Then we develop a smartphone based testbed and conduct a real experiment

by using this testbed to validate the EE performance of the proposed scenario.

- To broaden the scope of our work, we reveal a structure which can accommodate AI or machine learning based approaches to improve our work. It is well known that, AI or machine learning based approaches can be used to provide alternative ways to solve some difficult problems which are not well solved in the past. Therefore, in this work, we illustrate the structure which can accommodate this kind of approach to solve the problem mentioned in this paper.

The organization of this paper is shown as follows. The machine learnable bandwidth allocation strategy based wireless forwarding systems with the use of user cooperation and the assumptions about channel attenuation model are described in Sec. II. In Sec. III, for both non-cooperative and cooperative scenarios, we firstly derive two kinds of capacity expressions by using the mentioned channel attenuation models, and then calculate the approximate results for transmission power with the help of these expressions. In Sec. IV, we further calculate the power consumption by introducing a recent smartphone based power model. In Sec. V, we summarize some key findings after presenting some analysis results. In Sec. VI, a smartphone test-bed based experiment is conducted to veridate aforementioned analysis results. Discussion about how to use machine learning approaches in the studied topic is described in Sec. VII. Finally, some concluding remarks are given in Sec. VIII.

Notation: In order to denote matrices and vectors, in this paper, we use uppercase and lowercase boldface, respectively. The (i, j)th element of a matrix $\boldsymbol{A}$ is denoted by $[\boldsymbol{A}]_{ij}$, and the $n \times n$ identity matrix is denoted by I_n. The determinant of matrix $\boldsymbol{A}$ is given by $\det(\boldsymbol{A})$, and the expectation value operator is written as $\mathbb{E}\{\cdot\}$. In order to denote an integer collection, we use calligraphic font $\mathcal{A}$ and $|\mathcal{A}|$ to indicate the size of this collection. $\mathbb{C}^{m\times n}$ and $\mathbb{R}^{m\times n}$ denote the $m \times n$ dimensional complex and real matrix space. The symbols $(\boldsymbol{A})^*$ and $(\boldsymbol{A})^{\mathrm{H}}$ represent the transpose and Hermitian transpose of matrix $\boldsymbol{A}$, respectively.

II. SYSTEM AND CHANNEL MODEL

A. SYSTEM DESCRIPTION AND MACHINE LEARNABLE BANDWIDTH ALLOCATION STRATEGY

In this study, it is assumed that, there are a set $\mathcal{U} := \{1, \cdots, U\}$ of MTs (indexed with $u \in \mathcal{U}$) and a BS existing in the system. Further, the MTs are in close proximity of each other, and can communicate with the BS. Each MT is equipped with single antenna while the BS is equipped with M antennas. The communications among BS and MTs use an allocated bandwidth or spectrum resource B and can operate data forwarding. Each MT has two radio interfaces which can operate cellular and D2D transmissions. That is, one interface is for sending data to the BS, in other words, the cellular link, and the other one is for local data exchange with the other MTs, in other words, the D2D link.

In the traditional non-cooperative transmission scenario, it is assumed that, each MT directly sends its communication demand $C_u\, \forall u$ to the BS via the equally allocated non-overlapping bandwidth B/U. In the proposed cooperative transmission scenario, a proxy, which is selected from the MT set $\mathcal{U}$, works as an aggregator and sends the total traffic demands $C = \sum_{u=1}^{U}$ to the BS via a partial bandwidth νB by the cellular link. Other MTs, which are also called clients, occupy the remaining non-overlapping bandwidth resource of $(1-\nu)B$ equally to communicate with the proxy by the use of multiple D2D links.

In the aforementioned bandwidth allocation strategy, since ν is a proportion coefficient ranged from 0 to 1, based on the classical Shannon's information theory, two extreme cases of 0 and 1 will result in that transmit power at clients and proxy goes to infinity. Therefore, we can infer that, there exists an optimal ν value which can minimize the consumption power of the whole system, and this optimal ν value indirectly varies with the selected proxy and uplink CSI of MTs. This fact therefore enables system simplification and characteristic improvement by the machine learning approaches. In brief, we can use the position and demand information of each MT, to train neural networks of predicting proxy and bandwidth proportion coefficient ν. We leave the details of this machine learning approach described in Sec. VII, and an illustrations of the considered non-cooperative and cooperative transmission scenarios, the corresponding bandwidth allocation strategy are shown in Fig. 1.

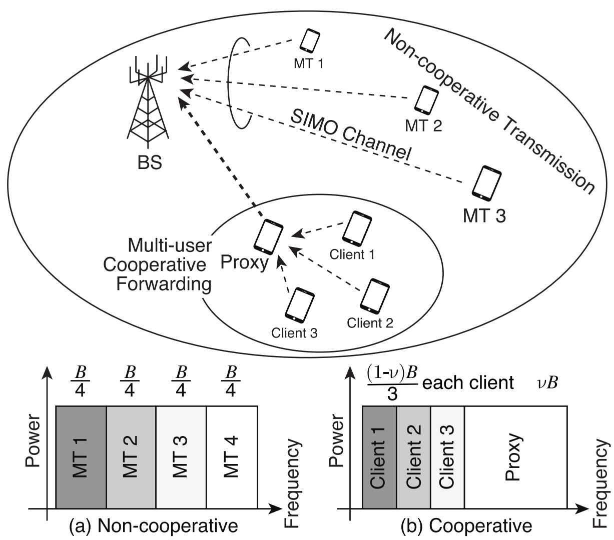

FIGURE 1. An example of the non-cooperative and cooperative scenarios under consideration and the related bandwidth allocation strategy for $U = 4$.

B. CHANNEL MODEL

In this system, we consider U single-input multiple-output (SIMO) wireless channels. Based on the results in [22], for a wireless system, if the maximum Doppler shift is very small when compared with the signal operation bandwidth, we can accurately convert each continuous-time

SIMO channel to discrete-time SIMO channel model with a proper delay and the channel can be expressed as

$$\boldsymbol{y}(t) = \sum_{l=0}^{L-1} \boldsymbol{h}(l,t)x(t-l) + \boldsymbol{n}(t), \tag{1}$$

where $t \in \{0, 1, \cdots, \infty\}$, $x(t) \in \mathbb{C}$ is the transmitted symbols, which comes from a zero-mean Gaussian codebook with unit average power. The noise term

$$\boldsymbol{n}(t) := (n_1(t), n_2(t), \cdots, n_M(t))^* \in \mathbb{C}^{M\times 1}$$

is zero-mean with $\mathbb{E}\{\boldsymbol{n}(t)\boldsymbol{n}^{\mathrm{H}}(t)\} = N_0 \mathrm{I}_M \,\forall t$, where N_0 is the noise power per Hertz. The output can be expressed as

$$\boldsymbol{y}(t) := (y_1(t), y_2(t), \cdots, y_M(t))^* \in \mathbb{C}^{M\times 1},$$

and we denote L as the channel length which is depending on the receive filter, the transmit filter, and the delay spread power profiles. It should be noted that the channel attenuation model becomes frequency flat model when the conditions of $L = 1$ is established.

$\boldsymbol{h}(l,t) \in \mathbb{C}^{M\times 1}$ is the lT_{s} (T_{s} is symbol period) delayed channel vector at time instant t and defined by

$$\boldsymbol{h}(l,t) := (h_1(l,t), h_2(l,t), \cdots, h_M(l,t))^*,$$

where $h_m(l,t)$ is the mth sub-channel's lth tap coefficient with time-varying index t, and can be written as

$$h_m(l,t) = \left(d^{-\zeta} 10^{\frac{s}{10}}\right)^{\frac{1}{2}} r_m(l,t), \tag{2}$$

where the path loss coefficient is modeled as $d^{-\zeta}$, and d is used to denote the distance between BS and MT, ζ is defined as the exponent of path loss.

We further use $s \in \mathbb{R}$ in decibel to represent the shadowing random variable (RV) from a MT to M BS antennas, and consider it follows the Gaussian distribution with mean μ and variance σ^2. In the present study, M shadowing RVs for all of MTs are spatially correlated with an exponentially correlated matrix $\boldsymbol{\Theta}_{\mathrm{s}} \in \mathbb{R}^{M\times M}$ without loss of generality, where the (u, u')th element is calculated by

$$[\boldsymbol{\Theta}_{\mathrm{s}}]_{uu'} = \exp\left(-\frac{d_{uu'}}{d_{\mathrm{cor}}}\ln 2\right), \tag{3}$$

where d_{cor} is correlation distance [23], [24], and $d_{uu'}$ is the distance between MT u and MT u'.

It should be noted that, the term $r_m(l,t) \in \mathbb{C}$ captures the small-scale fading attenuation, i.e., Rayleigh fading, which is modeled as independent and identically distributed (i.i.d) complex Gaussian RVs with zero mean and unit variance for all of MTs and all of the M BS antennas. The reason why we adopt this setting is because the distances among the MTs and BS antennas are separated enough geographically, which means generally they are all separated with distance more than half the operation wavelength. However, due to the convolution effects among the receive matched filter, transmit pulse shaping filter, and physical fading channel, discrete-time sampled channel $r_m(l,t)$ generally have inter-tap correlations. That means, the RVs $r_m(l,t)$ and $r_m(l',t)$ for $l \neq l'$ are correlated with an inter-symbol interference (ISI) inter-tap correlation coefficient matrix $\boldsymbol{\Theta}_{\mathrm{ISI}}$.

III. TRANSMISSION POWER CALCULATION

A. CAPACITY OVER FREQUENCY SELECTIVE CHANNELS

As the frequency selective channel attenuations are considered, it is necessary to analyzed the channel capacity based on a block of T output symbols at receiver (or BS in this case). The SIMO channel with ISI can be expressed as

$$\boldsymbol{Y} = \boldsymbol{H}\boldsymbol{x} + \boldsymbol{N}, \tag{4}$$

where

$$\begin{aligned}
\boldsymbol{Y} &:= \left(\boldsymbol{y}^*(t+1), \boldsymbol{y}^*(t+2), \cdots, \boldsymbol{y}^*(t+T)\right)^* \in \mathbb{C}^{MT\times 1},\\
\boldsymbol{x} &:= (x(t+T), x(t+T-1), \cdots, x(t-L+2))^* \\
&\qquad \in \mathbb{C}^{(T+L-1)\times 1},\\
\boldsymbol{N} &:= \left(\boldsymbol{n}^*(t+1), \boldsymbol{n}^*(t+2), \cdots, \boldsymbol{n}^*(t+T)\right)^* \in \mathbb{C}^{MT\times 1},\\
\boldsymbol{H} &:= \left(\boldsymbol{H}_1^*, \boldsymbol{H}_2^*, \cdots, \boldsymbol{H}_T^*\right)^* \in \mathbb{C}^{MT\times(T+L-1)},
\end{aligned}$$

and $\boldsymbol{H}_\tau \,\forall\tau \in \{1, \cdots, T\}$ is written as

$$\boldsymbol{H}_\tau := \big(\overbrace{\boldsymbol{0},\cdots,\boldsymbol{0}}^{\tau-1}, \overbrace{\boldsymbol{h}(L-1,t+\tau),\cdots,\boldsymbol{h}(0,t+\tau)}^{L}, \overbrace{\boldsymbol{0},\cdots,\boldsymbol{0}}^{T-\tau}\big). \tag{5}$$

In this study, two types of ergodic capacities which are used in non-cooperative and cooperative transmission scenarios are considered, respectively. From the results in Shannon's information theory, if the channel $\boldsymbol{H}$ are perfectly known to the BS for a large $T \gg L$, the ergodic capacity of a SIMO channel without use of cooperative transmission can be expressed as

$$C_{\mathrm{ns}} = \mathbb{E}\left\{\lim_{T\to\infty}\frac{B}{T}\log_2\det\left(\mathrm{I}_{TM} + \frac{P_{\mathrm{t}} d^{-\zeta} 10^{\frac{s}{10}}}{N_0 B}\boldsymbol{R}\boldsymbol{R}^{\mathrm{H}}\right)\right\}, \tag{6}$$

where P_{t} denotes transmission power, $\boldsymbol{R}$ represents the Rayleigh fading matrix which has the same form as $\boldsymbol{H}$ with a replacement of $\boldsymbol{h}(l,t)$ to $\boldsymbol{r}(l,t)$. The $\boldsymbol{r}(l,t)$ can be defined as

$$\boldsymbol{r}(l,t) := (r_1(l,t), r_2(l,t), \cdots, r_M(l,t))^* \in \mathbb{C}^{M\times 1}.$$

The capacity used in cooperative forwarding scenario is derived with the fact that the channel with best condition is selected and used. When a MT with best channel condition is selected as proxy, the ergodic capacity of the SIMO channel for this MT can be written as

$$C_{\mathrm{s}} = \mathbb{E}\left\{\lim_{T\to\infty}\frac{B}{T}\log_2\det\left(\mathrm{I}_{TM} + \frac{P_{\mathrm{t}}}{N_0 B}\hat{\boldsymbol{H}}\hat{\boldsymbol{H}}^{\mathrm{H}}\right)\right\}, \tag{7}$$

where $\hat{\boldsymbol{H}} := \left(\boldsymbol{H}_{1,\hat{u}_1}, \boldsymbol{H}_{2,\hat{u}_2}, \cdots, \boldsymbol{H}_{T,\hat{u}_T}\right)^*$, and $\hat{u}_\tau \,\forall\tau$ is decided by

$$\hat{u}_\tau = \arg\max_{u\in\mathcal{U}}\left(\mathrm{tr}\left(\boldsymbol{H}_{\tau,u}\boldsymbol{H}_{\tau,u}^{\mathrm{H}}\right)\right). \tag{8}$$

$\boldsymbol{H}_{\tau,u}$ denotes the channel sub-matrix defined in (5) for MT u.

Theorem 1: Under the effect of a frequency selective SIMO channel, for non-cooperative transmission scenario, if the transmission and its L sub-channels are also affected by the shadowing and spatially i.i.d. Rayleigh fading, then its ergodic capacity is given by (9), as shown at the bottom of this page, where

$$\Phi(\omega) = 1+2\sum_{i=1}^{L-1}\cos(i\omega)\left(\sum_{l=0}^{L-1-i}\mathbf{\Theta}_{\mathrm{ISI}}(l, l+i)\right), \quad (11)$$

and the coefficient $\mathbf{\Theta}_{\mathrm{ISI}}(l, l')$ is related to the channel fading power delay profile, the transmit filter, and the receive filter, and can be further simply calculated by (17) of [22].

Proof: For brevity, we defer the proof in **Appendix A**. ■

Theorem 2: With the consideration of U frequency selective SIMO channels with channel selection, for cooperative transmission forwarding scenario, if each SIMO channel and its L sub-channels experience spatially i.i.d. Rayleigh fading and spatially correlated shadowing with correlation matrix $\mathbf{\Theta}_{\mathrm{s}}$, then the ergodic capacity is given by (10), as shown at the bottom of this page, where $\Phi(\omega)$ is given by (11), $f_{\lambda_u}(\lambda)$, $F_{\lambda_u}(\lambda)$ can be calculated by the following expression

$$f_{\lambda_u}(\lambda) = \frac{\hat{d}_u^{-M}\lambda^{M-1}\mathrm{e}^{-\hat{d}_u^{-1}\lambda}}{(M-1)!} \quad (12)$$

and

$$F_{\lambda_u}(\lambda) = 1 - \sum_{m=0}^{M-1}\frac{1}{m!}\mathrm{e}^{-\hat{d}_u^{-1}\lambda}\left(\hat{d}_u^{-1}\lambda\right)^m, \quad (13)$$

where $\hat{d}_u$ is the normalized path loss of MT u and is obtained by $\hat{d}_u = d_u^{-\zeta}/||\boldsymbol{d}||$, $\boldsymbol{d} := (d_1^{-\zeta}, d_2^{-\zeta}, \cdots, d_U^{-\zeta})^* \in \mathbb{R}^{U\times 1}$. s_u is given by

$$s_u = \sqrt{2}\sum_{u'=1}^{U}\xi_{uu'}z_{u'} + \mu_u, \quad (14)$$

where $\xi_{uu'}$ is the (u, u')th element of Ξ_{sq} and $\Xi = \Xi_{\mathrm{sq}}\Xi_{\mathrm{sq}}^{\mathrm{H}}$. Ξ is the covariance matrix of U shadowing RVs and its (u, u')th element is calculated by $[\Xi]_{uu'} = \sigma_u\sigma_{u'}[\mathbf{\Theta}_{\mathrm{s}}]_{uu'}$. μ_u and σ_u^2 is the mean and variance of shadowing RV on uth MT.

Proof: For brevity, we defer the proof in **Appendix B**. ■

B. APPROXIMATION ON TRANSMISSION POWER

In the above subsection, two types of ergodic capacities which are corresponding to, (a) non-cooperative transmission scenario, (b) cooperative transmission scenario with the use of the best channel selection under the channel effects of frequency selective channels, are derived. Because it is difficult to calculate transmit power P_{t} from these complicated mathematical expressions of capacity, here we try to approximate the expressions of transmit power for practical use.

$$C_{\mathrm{ns}} = \frac{B}{2\pi^{\frac{3}{2}}(M-1)!}\int_0^{2\pi}\int_0^{\infty}\int_{-\infty}^{\infty}\lambda^{M-1}\mathrm{e}^{-(\lambda+s^2)}\log_2\left(1+\frac{P_{\mathrm{t}}d^{-\zeta}}{N_0B}10^{\frac{\sqrt{2}\sigma s+\mu}{10}}\Phi(\omega)\lambda\right)\mathrm{d}s\mathrm{d}\lambda\mathrm{d}\omega \quad (9)$$

$$\begin{aligned}C_{\mathrm{s}} = {}& \frac{B}{2\pi^{\left(1+\frac{U}{2}\right)}}\int_0^{2\pi}\int_0^{\infty}\int_{-\infty}^{\infty}\cdots\int_{-\infty}^{\infty}\exp\left(-\sum_{u=1}^{U}|z_u|^2\right)\log_2\left(1+\frac{P_{\mathrm{t}}||\boldsymbol{d}||\Phi(\omega)}{N_0B}\lambda\right)\left(\sum_{u=1}^{U}10^{-\frac{s_u}{10}}f_{\lambda_u}\right.\\ & \left.\left(10^{-\frac{s_u}{10}}\lambda\right)\prod_{k=1,k\neq u}^{U}F_{\lambda_k}\left(10^{-\frac{s_k}{10}}\lambda\right)\right)\prod_{u=1}^{U}\mathrm{d}z_u\mathrm{d}\lambda\mathrm{d}\omega \quad (10)\end{aligned}$$

$$P_{\mathrm{t,ns}}^{\mathrm{dBm}} \approx 10\log_{10}^{N_0B2^{\frac{C_{\mathrm{ns}}}{B}}} - \frac{\kappa}{\sqrt{\pi}(M-1)!}\sum_{n^{\mathcal{G}}=1}^{N^{\mathcal{G}}}\sum_{n^{\mathcal{H}}=1}^{N^{\mathcal{H}}}\sum_{n^{\mathcal{L}}=1}^{N^{\mathcal{L}}}\beta_{n^{\mathcal{G}}}^{\mathcal{G}}\beta_{n^{\mathcal{H}}}^{\mathcal{H}}\beta_{n^{\mathcal{L}}}^{\mathcal{L}}\left(\alpha_{n^{\mathcal{L}}}^{\mathcal{L}}\right)^{M-1}\log_2\left(\alpha_{n^{\mathcal{L}}}^{\mathcal{L}}d^{-\zeta}10^{\frac{\sqrt{2}\sigma\alpha_{n^{\mathcal{H}}}^{\mathcal{H}}+\mu}{10}}\Phi\left(2\pi\alpha_{n^{\mathcal{G}}}^{\mathcal{G}}\right)\right) \quad (16)$$

$$\begin{aligned}P_{\mathrm{t,s}}^{\mathrm{dBm}} \approx {}& 10\log_{10}^{N_0B2^{\frac{C_{\mathrm{s}}}{B}}} - \kappa\sum_{n^{\mathcal{G}}=1}^{N^{\mathcal{G}}}\sum_{n^{\mathcal{L}}=1}^{N^{\mathcal{L}}}\beta_{n^{\mathcal{G}}}^{\mathcal{G}}\beta_{n^{\mathcal{L}}}^{\mathcal{L}}\mathrm{e}^{\alpha_{n^{\mathcal{L}}}^{\mathcal{L}}}\log_2\left(\alpha_{n^{\mathcal{L}}}^{\mathcal{L}}||\boldsymbol{d}||\Phi\left(2\pi\alpha_{n^{\mathcal{G}}}^{\mathcal{G}}\right)\right)\sum_{n_1=1}^{N^{\mathcal{H}}}\cdots\sum_{n_U=1}^{N^{\mathcal{H}}}\left(\prod_{u=1}^{U}\frac{\beta_{n_u}^{\mathcal{H}}}{\sqrt{\pi}}\right)\left(\sum_{u=1}^{U}10^{-\frac{q_u}{10}}f_{\lambda_u}\right.\\ & \left.\left(10^{-\frac{q_u}{10}}\alpha_{n^{\mathcal{L}}}^{\mathcal{L}}\right)\prod_{k=1,k\neq u}^{U}F_{\lambda_k}\left(10^{-\frac{q_k}{10}}\alpha_{n^{\mathcal{L}}}^{\mathcal{L}}\right)\right) \quad (17)\end{aligned}$$

$$\begin{aligned}P_{\mathrm{t,s\text{-}c.c.}}^{\mathrm{dBm}} \approx {}& 10\log_{10}^{N_0B2^{\frac{C_{\mathrm{s\text{-}c.c.}}}{B}}} - \frac{\kappa}{\sqrt{\pi}}\sum_{n^{\mathcal{G}}=1}^{N^{\mathcal{G}}}\sum_{n^{\mathcal{H}}=1}^{N^{\mathcal{H}}}\sum_{n^{\mathcal{L}}=1}^{N^{\mathcal{L}}}\beta_{n^{\mathcal{G}}}^{\mathcal{G}}\beta_{n^{\mathcal{H}}}^{\mathcal{H}}\beta_{n^{\mathcal{L}}}^{\mathcal{L}}\mathrm{e}^{\alpha_{n^{\mathcal{L}}}^{\mathcal{L}}}\log_2\left(\alpha_{n^{\mathcal{L}}}^{\mathcal{L}}||\boldsymbol{d}||10^{\frac{\sqrt{2}\sigma\alpha_{n^{\mathcal{H}}}^{\mathcal{H}}+\mu}{10}}\Phi\left(2\pi\alpha_{n^{\mathcal{G}}}^{\mathcal{G}}\right)\right)\\ & \left(\sum_{u=1}^{U}f_{\lambda_u}\left(\alpha_{n^{\mathcal{L}}}^{\mathcal{L}}\right)\prod_{k=1,k\neq u}^{U}F_{\lambda_k}\left(\alpha_{n^{\mathcal{L}}}^{\mathcal{L}}\right)\right) \quad (18)\end{aligned}$$

Proposition 1: For scenario (a) and (b), the expressions of transmit power in decibel-milliwatts (dBm) can be approximately calculated by (16) and (17), as shown at the bottom of the previous page, respectively, where $\Phi(\omega)$ is given by (11), $f_{\lambda_u}(\lambda)$, $F_{\lambda_u}(\lambda)$ can be obtained by (12) and (13).

$$q_u = \sqrt{2}\sum_{j=1}^{U} \xi_{uj}\alpha_{n_j}^{\mathcal{H}} + \mu_u, \tag{15}$$

and $\kappa = 10\log_{10}^2$. $N^{\mathcal{G}}$, $N^{\mathcal{H}}$ and $N^{\mathcal{L}}$ are the Gauss, Gauss-Hermite and Gauss-Laguerre quadrature order. The abscissas $\alpha^{\mathcal{G}}$ and the associated weights $\beta^{\mathcal{G}}$ of Gauss quadrature for $N^{\mathcal{G}}$ up to 8, the abscissas $\alpha^{\mathcal{H}}$ and the associated weights $\beta^{\mathcal{H}}$ of Hermite quadrature for $N^{\mathcal{H}}$ up to 20, and the abscissas $\alpha^{\mathcal{L}}$ and the associated weights $\beta^{\mathcal{L}}$ of Laguerre quadrature for $N^{\mathcal{L}}$ up to 15 are tabulated in [27].

Proof: For brevity, we defer the proof in **Appendix C**. ∎

Proposition 2: For the most probable case that all MTs are affected by the completely correlated (c.c.) shadowing with mean μ and variance σ^2, the transmit power in dBm in scenario (b) can be approximately calculated by (18), as shown at the bottom of the previous page.

Proof: For brevity, we defer the proof in **Appendix D**. ∎

It should be noted that, the sum of transmit power and channel gain in dBm is the average receive power and it can be mathematically calculated by

$$P_{\mathrm{r},i}^{\mathrm{dBm}} \approx \frac{10C_i}{B}\log_{10}^2 + 10\log_{10}(N_0 B), \tag{19}$$

where i is ns, s, or s-c.c. corresponding to the mentioned different cases.

IV. POWER CONSUMPTION MODEL AND CALCULATION

A. POWER CONSUMPTION MODEL

To make our work more convincing, in this study, the LTE model of smartphones is adopted to evaluate the total consumed power of each MT approximately. Based on the model specified in [28], the consumed power of the MT which links to a cellular network is affected by the transmit as well as receive power levels, the modulation and coding scheme (MCS), and the data rate. In general, the consumed power in Watt of each MT can be expressed as

$$\begin{aligned} P_{\mathrm{con}} &= P_{\mathrm{on}} + \eta_{\mathrm{Rx}} \times \left(P_{\mathrm{Rx}} + P_{\mathrm{RxBB}}\left(C_{\mathrm{Rx}}^{\mathrm{M}}\right) + P_{\mathrm{RxRF}}\left(P_{\mathrm{r}}^{\mathrm{dBm}}\right)\right) \\ &\quad + \eta_{\mathrm{Tx}} \times \left(P_{\mathrm{Tx}} + P_{\mathrm{TxBB}}\left(C_{\mathrm{Tx}}^{\mathrm{M}}\right) + P_{\mathrm{TxRF}}\left(P_{\mathrm{t}}^{\mathrm{dBm}}\right)\right), \end{aligned} \tag{20}$$

where η_{Rx} and η_{Tx} are binary variables representing whether the MT is receiving or transmitting. The constants P_{on}, P_{Rx}, and P_{Tx} are the consumption power of the cellular network, the receiver, and the transmitter, respectively. P_{RxBB}, P_{TxBB}, P_{RxRF}, and P_{TxRF} are liner functions of rate and power which are listed in the TABLE 1 [28]. In the following, we evaluate consumed power of the MTs for different scenarios.

TABLE 1. Consumption power in mW [28].

Part	Polynomial	Comment
P_{on}	853	Cellular active
P_{Rx}	25.1	Receive active
P_{Tx}	29.9	Transmit active
$P_{\mathrm{RxBB}}(C_{\mathrm{Rx}}^{\mathrm{M}})$	$0.97C_{\mathrm{Rx}}^{\mathrm{M}} + 8.16$	–
$P_{\mathrm{RxRF}}(P_{\mathrm{r}}^{\mathrm{dBm}})$	$-0.04P_{\mathrm{r}}^{\mathrm{dBm}} + 24.8$	$P_{\mathrm{r}}^{\mathrm{dBm}} \leqslant -52.5$dBm
$P_{\mathrm{RxRF}}(P_{\mathrm{r}}^{\mathrm{dBm}})$	$-0.11P_{\mathrm{r}}^{\mathrm{dBm}} + 7.86$	$P_{\mathrm{r}}^{\mathrm{dBm}} > -52.5$dBm
$P_{\mathrm{TxBB}}(C_{\mathrm{Tx}}^{\mathrm{M}})$	0.62	–
$P_{\mathrm{TxRF}}(P_{\mathrm{t}}^{\mathrm{dBm}})$	$0.78P_{\mathrm{t}}^{\mathrm{dBm}} + 23.6$	$P_{\mathrm{t}}^{\mathrm{dBm}} \leqslant 0.2$ dBm
$P_{\mathrm{TxRF}}(P_{\mathrm{t}}^{\mathrm{dBm}})$	$17P_{\mathrm{t}}^{\mathrm{dBm}} + 45.4$	$0.2 < P_{\mathrm{t}}^{\mathrm{dBm}} \leqslant 11.4$ dBm
$P_{\mathrm{TxRF}}(P_{\mathrm{t}}^{\mathrm{dBm}})$	$5.9\left(P_{\mathrm{t}}^{\mathrm{dBm}}\right)^2 - 118P_{\mathrm{t}}^{\mathrm{dBm}} + 1195$	$P_{\mathrm{t}}^{\mathrm{dBm}} > 11.4$ dBm

B. POWER CONSUMPTION CALCULATION

It is straightforward to know that, the total power consumption $P_{\mathrm{con}}^{\mathrm{cell}}$ of U MTs in cellular system without user cooperation is the sum of consumed power per MT with SIMO transmission in cellular system. Therefore, we have:

$$P_{\mathrm{con}}^{\mathrm{cell}} = \sum_{u=1}^{U}\left(P_{\mathrm{c}_1} + P_{\mathrm{TxBB}}\left(C_0^{\mathrm{M}}\right) + P_{\mathrm{TxRF}}\left(P_{\mathrm{t,ns},u}^{\mathrm{dBm}}\left(C_0, \frac{B}{U}\right)\right)\right), \tag{21}$$

where $P_{\mathrm{c}_1} = P_{\mathrm{on}} + P_{\mathrm{Tx}}$, and $P_{\mathrm{con}}^{\mathrm{cell}}$ is calculated by (20) for $\eta_{\mathrm{Rx}} = 0$ and $\eta_{\mathrm{Tx}} = 1$, $C_{\mathrm{Tx}}^{\mathrm{M}} = C_0 \,\forall u \in \mathcal{U}$ in Mbps are the capacities in the cellular links, and $P_{\mathrm{t}}^{\mathrm{dBm}} = P_{\mathrm{t,ns},u}^{\mathrm{dBm}}$ is the transmission power level of MT u and be calculated by (16) for $C_{\mathrm{ns}} = C_0$, $B = B/U$, and the associated channel attenuations.

The total power consumption $P_{\mathrm{con}}^{\mathrm{coop}}$ for cooperative transmission forwarding is a function of the power consumption of the clients $P_{\mathrm{con}}^{\mathrm{clients}}$ and proxy $P_{\mathrm{con}}^{\mathrm{proxy}}$. Therefore, we have the following expression:

$$P_{\mathrm{con}}^{\mathrm{coop}} = P_{\mathrm{con}}^{\mathrm{clients}} + P_{\mathrm{con}}^{\mathrm{proxy}}, \tag{22}$$

where $P_{\mathrm{con}}^{\mathrm{clients}}$ and $P_{\mathrm{con}}^{\mathrm{proxy}}$ can be expressed as

$$\begin{aligned} P_{\mathrm{con}}^{\mathrm{clients}} &= \sum_{u\in\mathcal{U}, u\neq u_p} (P_{\mathrm{c}_1} + P_{\mathrm{TxBB}}(C_0^{\mathrm{M}}) \\ &\quad + P_{\mathrm{TxRF}}(P_{\mathrm{t,ns\text{-}c},u}^{\mathrm{dBm}}(C_0, \frac{\nu B}{U-1}))) \end{aligned} \tag{23}$$

and

$$\begin{aligned} &P_{\mathrm{con}}^{\mathrm{proxy}} \\ &= P_{\mathrm{c}_2} + P_{\mathrm{RxBB}}\left((U-1)C_0^{\mathrm{M}}\right) + P_{\mathrm{RxRF}}\left(P_{\mathrm{r,ns}}^{\mathrm{dBm}}\left((U-1)C_0, \nu B\right)\right) \\ &\quad + P_{\mathrm{TxBB}}\left(UC_0^{\mathrm{M}}\right) + P_{\mathrm{TxRF}}\left(P_{\mathrm{t},i}^{\mathrm{dBm}}\left(UC_0, (1-\nu)B\right)\right), \end{aligned} \tag{24}$$

where $P_{\mathrm{c}_2} = P_{\mathrm{on}} + P_{\mathrm{Tx}} + P_{\mathrm{Rx}}$, and u_{p} in (23) denotes the index of proxy. $P_{\mathrm{con}}^{\mathrm{clients}}$ is calculated by (20) for $\eta_{\mathrm{Rx}} = 0$ and $\eta_{\mathrm{Tx}} = 1$, $C_{\mathrm{Tx}}^{\mathrm{M}} = C_0 \,\forall u$ in Mbps are the capacities of the client-to-proxy links, and $P_{\mathrm{t}}^{\mathrm{dBm}} = P_{\mathrm{t,ns\text{-}c},u}^{\mathrm{dBm}}$ is the transmission power level of client u and can be evaluated by expression (16) for $C_{\mathrm{ns}} = C_0$, $B = \nu B/(U-1)$, and the associated channel effects from client u to proxy.

$P_{\mathrm{con}}^{\mathrm{proxy}}$ is also obtained by (20) for $\eta_{\mathrm{Rx}} = 1$ and $\eta_{\mathrm{Tx}} = 1$, $C_{\mathrm{Rx}}^{\mathrm{M}} = (U-1)C_0$ in Mbps is the sum of capacities over all of client-to-proxy links, $P_{\mathrm{r}}^{\mathrm{dBm}} = P_{\mathrm{r,ns}}^{\mathrm{dBm}}$ is the receive power level of the proxy in user cooperation aided transmission forwarding scenario and can be calculated by (19) for $C_{\text{ns}} = (U-1)C_0$, $B = \nu B$. $C_{\text{Tx}}^{\text{M}} = UC_0$ in Mbps is the sum capacity of all the MTs, and $P_{\text{t}}^{\text{dBm}} = P_{\text{t},i}^{\text{dBm}}$ is the transmit power level of proxy in cellular link, and can be calculated by (17) for $C_i = UC_0$, $B = (1-\nu)B$, and the associated channel attenuation from the proxy to BS in which i is s or s-c.c. corresponding to the effects of the generalized correlated or c.c. shadowing.

It should be noted that, with the assumption that user cooperation among MTs use less bandwidth or spectrum resource (referred by Fig. 3) because of their shorter transmission distances, and the consideration of rich scattered environment that is existing in local transmissions caused by the higher population density and complicated surroundings, in this study, we employ a flat (i.e., $L = 1$) Rayleigh fading attenuation model to calculate the consumption power for all of the clients for a worst-case of user cooperative transmission scenario.

In addition, in the case of the power consumption of the proxy $P_{\text{con}}^{\text{proxy}}$, the result of proxy selection has been included and therefore it can be evaluated directly. However, in the case of the power consumption of the clients $P_{\text{con}}^{\text{clients}}$, it is a RV which is varying according to the result of the proxy selection. As a result, it is difficult to evaluate the value of the power consumption $P_{\text{con}}^{\text{clients}}$. To resolve this problem with reasonable computational complexity, an average inter-MT distance $\bar{d}$ to approximate the power consumption of clients $P_{\text{con}}^{\text{clients}}$ is adopted with the assumption that shadowing between the clients and proxy follows the same distribution. Then we can obtain the following result:

$$P_{\text{con}}^{\text{clients}} \approx (U-1)\left(P_{\text{c}_1} + P_{\text{TxBB}}\left(C_0^{\text{M}}\right) + P_{\text{TxRF}}\left(P_{\text{t,ns-c}}^{\text{dBm}}\left(C_0, \frac{\nu B}{U-1}, \bar{d}\right)\right)\right), \tag{25}$$

where $P_{\text{t,ns-c}}^{\text{dBm}}$ is re-calculated by (16) for $C_{\text{ns}} = C_0$, $B = \nu B/(U-1)$, and $d = \bar{d}$. $\bar{d}$ is obtained by

$$\bar{d} = \frac{2}{U(U-1)} \sum_{u=1}^{U} \sum_{u'=u+1}^{U} d_{uu'}. \tag{26}$$

Finally, we can obtain $P_{\text{con}}^{\text{coop}}$ as an approximate sum of (24) and (25).

V. NUMERICAL RESULTS

To verify the theoretical results derived in Sec. III, some simulations, which employ the time-varying frequency selective fading channel model addressed in Sec. II, are conducted in this section. The simulation parameters are summarized and listed in TABLE 2.

In Fig. 2, the numerical results of two types of capacities evaluated by expressions (9) and (10) are shown. The results of arbitrary SIMO channel are evaluated by (9), and the results of SIMO channel using the best channel condition are obtained by (10). In both cases the results are evaluated

TABLE 2. Main configurations.

Parameters	Values
Num. of BS antennas	$M = 8$
Position and deployment of BS antennas	Centralized, (0, 0)
Central position of cooperative area	(1000, 0) m
Radius of cooperative area	20 m
Deployment of MTs in cooperative area	uniform distribution
Bandwidth	$B = 20$ MHz
Thermal noise	-174 dBm/Hz
Maximal transmit power	23 (D2D: 13) dBm
Exponent of path loss	$\zeta = 4$
Num. of subchannels	$L = 4$ ($L = 1$ for coop.)
ISI coeff. between l and l' sub-channel	$\mathbf{\Theta}_{\text{ISI}} = 0.95^{\lvert l-l' \rvert}/4$
Mean and var. of shad. for cellular	0 dB, 10 dB
Mean and var. of shad. for coop.	0 dB, 12 dB
Gauss, Hermite, and Laguerre orders	$N^{\mathcal{G}} = 8$, $N^{\mathcal{H}} = 12$, $N^{\mathcal{L}} = 12$

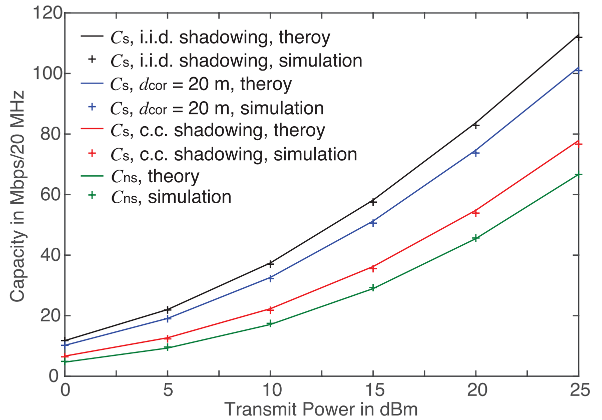

FIGURE 2. Simulated and theoretical capacity performance under the effects of varying shadowing correlations, $U = 4$.

with different correlations for shadowing. From the simulation results, it can be seen that, the theoretical expressions derived in Sec. III match the numerical simulation results quite well, which validates the effectiveness of the theoretical results and convinces that the theoretical expressions can be used in the evaluation of power consumption. However, because of the large computational cost for numerical simulations, since the theoretical results can well approximate the numerical simulation results, we show the theoretical results only without numerical simulation results in the following figures to save the computational resources.

The relationships between ν, which is configured in the proposed machine learnable bandwidth allocation strategy, and power consumption of cooperative forwarding scenario over the channel effects considered in this work with different traffic demand for each MT, are shown in Fig. 3. From the results in the figure, our inference that, there exists an optimal ν value which can minimize system power consumption, can be confirmed. Besides, it also indicates that using about 10% bandwidth resource into user cooperative transmission can approximately optimize the consumed power for the case of $C_0 = 15$ Mbps and $U = 4$.

In Fig. 4, some comparisons of power consumption for non-cooperative and cooperative scenarios are shown. The results are shown according to the varying number of MTs

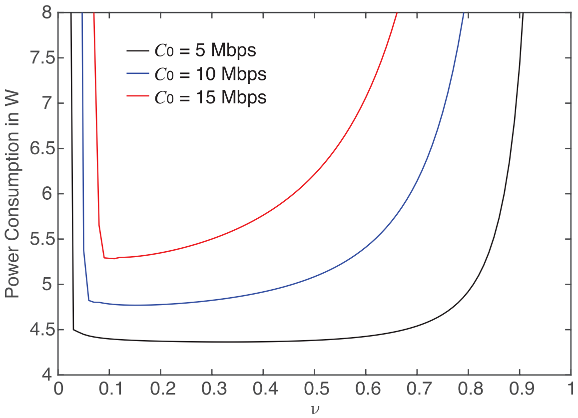

FIGURE 3. Relationship between band allocation proportion ν and power consumption in cooperative scenario with $U = 4$.

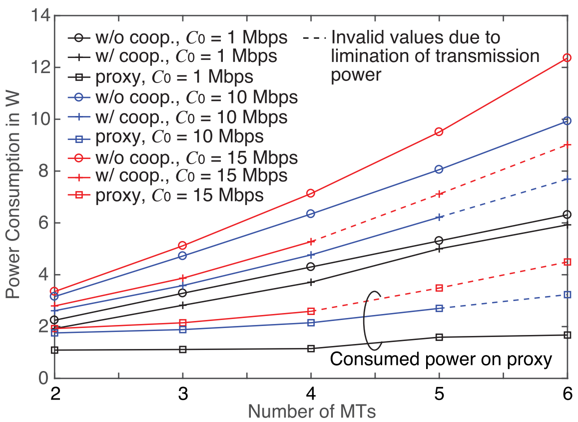

FIGURE 4. Comparisons of power consumption under non-cooperative and cooperative scenarios with the use of (16) and (18) under the effect of c.c. shadowing.

with different traffic demands for each MT. The power consumption of proxy is also shown in Fig. 4 as a benchmark. It should be noted that, the power consumption in cooperative case is evaluated by estimating an optimal value of ν.

From the results shown above, it can be seen that, the power consumption can be significantly reduced by using user cooperation aided forwarding technique over frequency selective fading channel, and the proportion of power consumption reduction is getting larger with the increase of total communication demand. However, there are also some points are needed to be noted.

First of all, because of the physical constraints applied on the proxy, for example, maximum transmit power, we cannot arbitrarily increase the total communication demand. This condition can be verified by that, the maximum number of the MTs working on the cooperative transmission scenario is limited with fixed communication demands, or decreases with the increase of the communication demand. Secondly, the results in Fig. 4 are evaluated with consideration of the worst channel attenuation case, in other words, all MTs are affected by the c.c. shadowing and hence the large-scale fading is approximately identical. In real cases, however, shadowing on each MT may be quite different because of the surrounding obstacles. As a result, the benefits of user cooperation aided transmission forwarding should be able to further improved. However, the MT with the best large-scale fading gain may be frequently selected as a proxy, and hence the energy consumed for traffic forwarding should be larger than other MTs. Therefore, several issues about fairness should be considered more carefully in related works.

VI. SMARTPHONE TEST-BED BASED EVALUATION

To further verify our analysis results in Fig. 4, in this section, we experimentally evaluate the EE improvement of non-cooperative and cooperative traffic forwarding scenarios by smartphone test-bed which follows from real communication standards. In this work, we use Wi-Fi and Bluetooth interfaces to transfer local data and share control information among MTs, respectively, and LTE link is created to communicate between the proxy and BS.

It is should be noted that, because only operator has the permissions to adjust the parameters of BS including working frequency and bandwidth, the proposed bandwidth allocation strategy cannot be directly adopted in the current experiments. However, considering that the bandwidth setting of the test-bed can be seen as a simplified version of the proposal with a fixed ν where νB is allocated to LTE link and $(1 - \nu)B$ is allocated to Wi-Fi and Bluetooth links, regardless the optimization issue, our experimental results still can be applied on general cases.

A. EXPERIMENT DESCRIPTION AND SETTING

In Fig. 5 the smartphone deployment are shown with different reference signal receive power (RSRP) following LTE standard. The RSRP information adopted in our experiments is used to imply that the distance between the service providing BS and experiment field, where small value of RSRP implies a large distance. In current indoor experiments, we used prepaid pack with 1 GB NanoSIM card (au 4G LTE compatible) which can provide mobile virtual network operator service via KDDI[1] LTE network to connect with LTE BS. There are totally three types of traffic forwarding scenarios adopted in the experiment, i.e., (a) non-cooperative case with two MTs, (b) cooperative case with two MTs, (c) same as (b) with four MTs, which are demonstrated in this experiment.

In addition, we also developed a novel smartphone application on Android operation system and installed this application on a Google smartphone *Nexus 5x* to process the cooperative operations among the MTs. For giving an intuitive understanding, in Fig. 6, an example of the application interface is shown. For the smartphone application used on the MTs, it can realize cooperative communications among MTs. Besides, it can also implement the operations that, one MT serves as proxy while other MTs can do communication via the MT which serves as proxy. The detail

[1] KDDI Corporation is a Japanese telecommunications operator which is established in October 1, 2000.

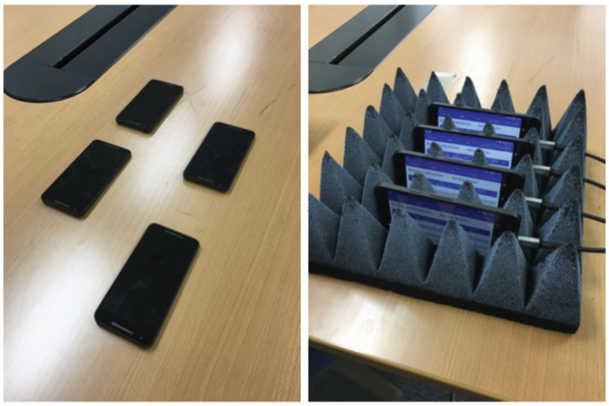

(a) LTE RSRP ≈ -85 dBm (b) LTE RSRP ≈ -105 dBm

FIGURE 5. **Smartphone/MT deployments used in the experiments. The LTE RSRP in (a) is about -85 dBm, and in (b) is about −105 dBm.**

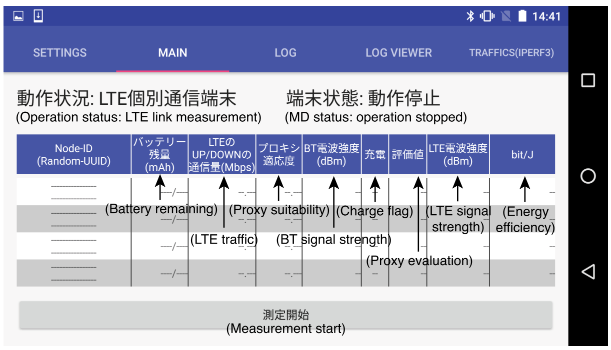

FIGURE 6. **Interface of the built application including SETTING, MAIN, LOG, LOG VIEWER, and TRAFFICS (IPERF3) panels. The screenshot shows the MAIN panel.**

TABLE 3. **Information detail in database.**

Parameters	Unit	Explanation
Node ID	–	Unique ID for each MT
Battery remaining	mAh	–
LTE traffic	bps	–
BT signal strength	dBm	RSRP on Bluetooth signal
Charge flag	–	Power charging indicator
Proxy evaluation	–	Indicate whether appropriate as proxy
LTE signal strength	dBm	RSRP on LTE signal
Energy efficiency	bit/J	–

information about the database is listed in TABLE 3. Besides, this information is also shown in the main interface of our self-developed smartphone application (please see Fig. 6).

Furthermore, each MT generates its communication demands using Iperf3 server and uploads the data via the LTE connection with scenario (a), or via the proxy with scenario (b)(c) under the user datagram protocol (UDP) mode. To simplify the workflow of measurements, we adopt the following three patterns of traffic demands in the experiment, i.e., $C_u = 1.4, 2.8, 7.0$ Mbps, for all of the MTs and all of the transmissions described above. For example, in (c), the total communication demand of the proxy is $C = \sum_{u=1}^{4} C_u = 5.6$ Mbps under the condition that the communication demand for each client is 1.4 Mbps.

Because the evaluation of the energy consumption without any hardware modification is hard, in our current experiments, a method that measure the reduction rate ρ of the battery capacity and thereby indirectly calculate the energy consumption is adopted. About the hardware specifications, the capacity of full charged battery for smartphone *Nexus 5x* is 2700 mAh and the rated voltage is referred as 3.8 V. By knowing this kind of information, the energy consumption E in joule caused by the wireless transmission therefore can be approximately calculated by the following expression:

$$E(\mathrm{J}) = 2700 \times 10^{-3}(\mathrm{Ah}) \times 3.8(\mathrm{V}) \times 3600(\mathrm{sec.}) \times \rho. \quad (27)$$

B. EXPERIMENT RESULTS

In this subsection, we evaluate the EE of both non-cooperative and cooperative traffic forwarding with the use of the proposed machine learnable bandwidth allocation strategy and show the results based on the aforementioned smartphone test-bed to validate the proposed method. The EE is defined as a value of total traffic demand divided by the system energy consumption.

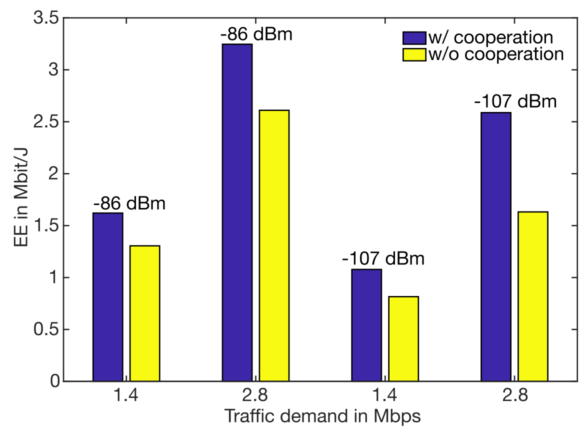

FIGURE 7. **Comparisons of the EEs of traffic forwarding (a) and (b) under the effects of different LTE RSRPs and different traffic demands.**

In Fig. 7, the results of EE performance under different traffic forwarding scenarios (a) and (b) are presented. These results are shown with different LTE RSRPs and $U = 2$. From the results in the figure, it can be seen that, in all the cases, the EE performance of cooperative transmission is improved minimally 24%. When the LTE RSRP equals to −107 dBm and the traffic demand equals to 2.8 Mbps, the EE performance is significantly improved by 58%. One of the reasons why the EE performance can be improved is that, the proximity communication, i.e., D2D links in our study, can save energy in a more effective way than cellular links do, due to its shorter transmission distance and larger probability of line-of-sight paths.

in Fig. 8, we compare the EE performance of forwarding scenario (c) with that of (b) under the same condition of LTE RSRP $= -86$ dBm and traffic demand of each MT $= 1.4$ Mbps. From the experiment results, it can be seen that, as we expected, the EE performance of cooperative

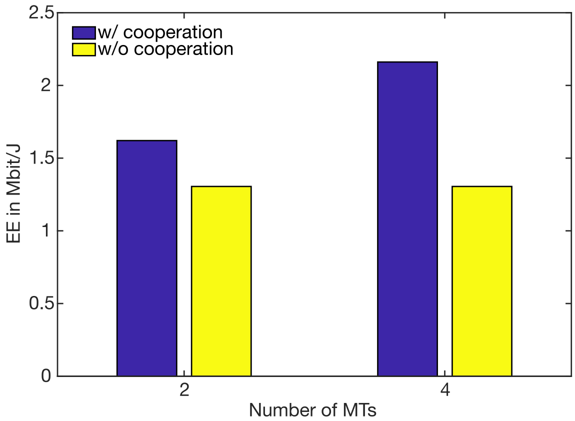

FIGURE 8. Comparisons of the EEs of traffic forwarding (b) and (c) under the effects of LTE RSRP = −86 dBm and traffic demand of each MT = 1.4 Mbps.

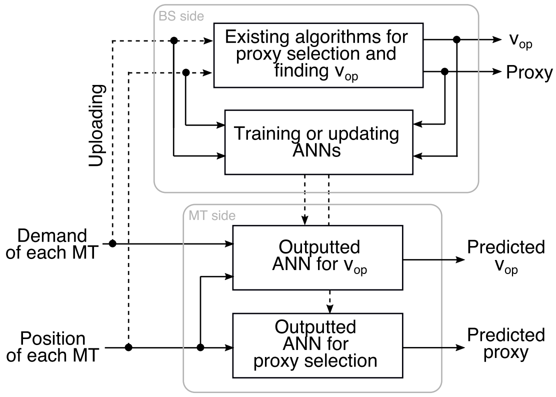

FIGURE 9. An illustration of ML aided proxy selection and ν_{op} prediction using neural network.

forwarding with four MTs is significantly increased by up to 66% energy-saving gain. Therefore, it can be known that our experiment results well match the findings of numerical analysis and consequently experimentally validate the potential improvement of the EE performance by the proposed method.

VII. DISCUSSION

From our analysis results in Sec. V, it can be known that, there exists an optimal value of ν which can minimize system power consumption. In order to find this optimal value ν_{op}, BS needs to collect the uploaded CSI and traffic demand of each MT, and perform a series of calculation tasks, which causes some delay and thus reduces communication efficiency. Because if we want to resolve this kind of tasks which are complex and computationally resource consuming, the past experience and available data are needed rather than using approaches based on explicit rules and instructions. Therefore, the machine learning approaches can be adopted in this study to reduce system complexity and improve transmission performances.

For instance, in Fig. 9, we show an illustration of machine learning aided proxy selection and ν_{op} prediction with the use of artificial neural networks[2] (ANNs) for the proposed cooperative traffic forwarding. By averaging the effects of small-scale fading, traditionally, each MT uploads its position and traffic demand to the BS, and the BS uses existing algorithms to select proxy and calculate ν_{op} with the help of these uploaded information. Then the results (proxy and ν_{op}) are fed backed to each MT and BS can performs follow-up operations.

Specifically, with machine learning approaches, BS can further utilize these previous information, i.e., proxy and ν_{op} obtained by the existing algorithms, to train or update ANNs which are used to predict the selection of proxy and ν_{op} without the existing algorithms. Once stable ANNs are established at BS side, the networks thereafter can be distributed to each MT by operator updates for instance. Then MTs use these trained or updated networks to select proxy and calculate ν_{op} (surely, error should be allowed). Finally, it is not necessary to upload MT's information to the BS and MTs can select a proxy (may not be accurate) and use the predicted ν_{op} to perform the cooperative traffic forwarding. That can result in reduction of system complexity and improvement of communication efficiency.

Certainly, there are still other aspects of problems which can be solved by machine learning approaches, and in the current study we provide a design framework which can introduce the machine learning related approaches to solve the problems. More related studies for cooperative communications are planned in our future works.

VIII. CONCLUSION

In this study, we proposed a simple and novel machine learnable bandwidth allocation strategy for user cooperation aided wireless communication systems, and evaluated the power consumption of the systems using theoretical and experimental methods in cellular network systems under the environment with frequency selective fading channels and spatially correlated shadowing. With the adoption of the proposed bandwidth allocation strategy, first of all we derived some theoretical expressions to evaluate the transmission power for non-cooperative and cooperative transmission scenarios, and then we mathematically analyzed the power consumption with the help of a recent LTE power model for smartphones, and finally evaluated the concluded results by our smartphone test-bed. From the numerical and experimental results, it can be seen that, the benefits of cooperative forwarding are significant. However, according to our analysis, it is difficult to be fully achieved in real environment because of some limitations, for example, maximum transmit power on MT. Furthermore, allocation of bandwidth resource dominated the transmission performances of user cooperation aided transmission forwarding and is strongly affected by, e.g., position and traffic demand of each MT. Machine learning approaches aided cooperative traffic forwarding can be used to reduce

[2]ANN is a computing systems vaguely inspired by the biological neural networks that constitute animal brains for solving machine learning problems.

the considered system complexity and improve transmission efficiency, which is also discussed in this study and left as one of the future topics.

APPENDIX A
PROOF OF THEOREM 1

Since the ergodic capacity is not affected by the time variation for ergodic fading channels, the theorem can be proved by considering the slow time-varying scenario. The Rayleigh fading matrix $\boldsymbol{R}$ in (6) can be viewed as a block Toeplitz matrix with the following expression $\boldsymbol{R} := (\boldsymbol{R}_1^*, \boldsymbol{R}_2^*, \cdots, \boldsymbol{R}_T^*)^* \in \mathbb{C}^{MT\times(T+L-1)}$, where

$$\boldsymbol{R}_\tau := (\overbrace{\boldsymbol{0}, \cdots, \boldsymbol{0}}^{\tau-1}, \overbrace{\boldsymbol{r}(L-1,t), \cdots, \boldsymbol{r}(0,t)}^{L}, \overbrace{\boldsymbol{0}, \cdots, \boldsymbol{0}}^{T-\tau}). \tag{28}$$

According to the property of the block Toeplitz matrix [25] and by the assumption that the Rayleigh fading and shadowing can be viewed as mutually independent random processes, from the results in [26], the ergodic capacity (6) averaged over spatially i.i.d. Rayleigh fading for SIMO channel without channel selection can be expressed as

$$C'_{\mathrm{ns}} = \frac{B}{2\pi(M-1)!}\int_0^\infty\int_0^{2\pi} \log_2\left(1+\frac{P_{\mathrm{t}}10^{\frac{s}{10}}}{d^\zeta N_0 B}\Phi(\omega)\lambda\right)\frac{\lambda^{M-1}}{\mathrm{e}^{-\lambda}}\mathrm{d}\omega\mathrm{d}\lambda. \tag{29}$$

Because of the fact that s is with normal distribution with mean μ and variance σ^2, by the help of the probability density function (PDF) of s which can be expressed as

$$f_s(s) = \frac{1}{\sqrt{2\pi\sigma^2}}\exp\left(-\frac{(s-\mu)^2}{2\sigma^2}\right), \tag{30}$$

we can conclude the proof.

APPENDIX B
PROOF OF THEOREM 2

By using the same approach addressed above and the fact that matrix $\hat{\boldsymbol{H}}$ in (7) is also a block Toeplitz matrix, from the results in [26] and by doing some simplification works, the capacity in (7) can be expressed by

$$C_{\mathrm{s}} = \frac{B}{2\pi}\int_0^{2\pi}\mathbb{E}\left\{\log_2\left(1+\frac{P_{\mathrm{t}}||\boldsymbol{d}||\Phi(\omega)}{N_0 B}\Lambda\right)\right\}\mathrm{d}\omega, \tag{31}$$

where

$$\Lambda = \max_{u\in\mathcal{U}} 10^{\frac{s_u}{10}}\lambda_u, \tag{32}$$

s_u means the shadowing between uth MT and BS, $\lambda_u = \hat{d}_u\sum_{m=1}^{M}|r_{u,m}|^2$, and $r_{u,m}\ \forall u, m$ is i.i.d. zero mean circularly symmetric complex Gaussian RVs.

Because of the fact that the shadowing varies slowly than the Rayleigh fading, and also by the assumption that shadowing and fading can be viewed as mutually independent random processes, consequently, for U MT diversity, the cumulative distribution function (CDF) of Λ can be expressed as

$$F_\Lambda(\lambda) = p\left(\max_{u\in\mathcal{U}}\left(10^{\frac{s_u}{10}}\lambda_u\right) < \lambda\right) = \prod_{u=1}^{U} p\left(10^{\frac{s_u}{10}}\lambda_u < \lambda\right). \tag{33}$$

Then the PDF of Λ by differentiating $F_\Lambda(\lambda)$ relative to λ and the outage probability by evaluating $F_\Lambda(\lambda)$ at $\lambda = \lambda_0$ can be obtained. Therefore, based on (33), the outage probability of RV Λ for the target λ_0 can be rewritten as

$$F_\Lambda(\lambda_0) = \int_{-\infty}^{\infty}\left(\prod_{u=1}^{U}F_{\lambda_u}\left(10^{-\frac{s_u}{10}}\lambda_0\right)\right)f_{\boldsymbol{S}}(\boldsymbol{s})\mathrm{d}\boldsymbol{s}, \tag{34}$$

where $f_{\boldsymbol{S}}(\boldsymbol{s})$ is the joint distribution of U correlated shadowing RVs, and $\boldsymbol{s}$ is defined as a vector consists of U shadowing RVs and is written as $\boldsymbol{s} = (s_1, s_2, \cdots, s_U)^*$.

When U Gaussian RVs, $\{s_u\}_{u=1}^{U}$, are correlated, the joint distribution $f_{\boldsymbol{S}}(\boldsymbol{s})$ is given by

$$f_{\boldsymbol{S}}(\boldsymbol{s}) = \frac{1}{(2\pi)^{\frac{U}{2}}\det(\boldsymbol{\Xi})^{\frac{1}{2}}}\exp\left(-\frac{(\boldsymbol{s}-\boldsymbol{\mu})^{\mathrm{H}}\boldsymbol{\Xi}^{-1}(\boldsymbol{s}-\boldsymbol{\mu})}{2}\right), \tag{35}$$

where $\boldsymbol{\Xi}$ is the covariance matrix and $\boldsymbol{\mu} = (\mu_1, \mu_2, \cdots, \mu_U)^*$ is the vector of means of the Gaussian RVs. (34) can then be written as

$$F_\Lambda(\lambda_0) = \int_{-\infty}^{\infty}\frac{1}{(2\pi)^{\frac{U}{2}}\det(\boldsymbol{\Xi})^{\frac{1}{2}}}\left(\prod_{u=1}^{U}F_{\lambda_u}\left(10^{-\frac{s_u}{10}}\lambda_0\right)\right) \times\exp\left(-\frac{(\boldsymbol{s}-\boldsymbol{\mu})^{\mathrm{H}}\boldsymbol{\Xi}^{-1}(\boldsymbol{s}-\boldsymbol{\mu})}{2}\right)\mathrm{d}\boldsymbol{s}. \tag{36}$$

Differentiating (36) relative to λ_0 with the use of product rule, the PDF of Λ is expressed as

$$f_\Lambda(\lambda) = \int_{-\infty}^{\infty}\frac{(2\pi)^{-\frac{U}{2}}}{\det(\boldsymbol{\Xi})^{\frac{1}{2}}}\left(\sum_{u=1}^{U}10^{-\frac{s_u}{10}}f_{\lambda_u}\left(10^{-\frac{s_u}{10}}\lambda\right)\prod_{k=1,k\neq u}^{U}F_{\lambda_k}\left(10^{-\frac{s_k}{10}}\lambda\right)\right) \times\exp\left(-\frac{(\boldsymbol{s}-\boldsymbol{\mu})^{\mathrm{H}}\boldsymbol{\Xi}^{-1}(\boldsymbol{s}-\boldsymbol{\mu})}{2}\right)\mathrm{d}\boldsymbol{s}, \tag{37}$$

where f_{λ_u} and F_{λ_u} are the PDF and CDF of RV λ_u, respectively. As the mutually independent RVs $\hat{d}_u|r_{u,m}|^2$ follow the exponential distribution with the same rate parameter $\hat{d}_u^{-1}$, their sum λ_u is the RV following the Erlang distribution with the corresponding PDF and CDF given by (12) and (13).

Thereafter, let $\boldsymbol{\Xi}_{\mathrm{sq}}$ be the square root of the covariance matrix $\boldsymbol{\Xi}$, i.e., $\boldsymbol{\Xi} = \boldsymbol{\Xi}_{\mathrm{sq}}\boldsymbol{\Xi}_{\mathrm{sq}}^{\mathrm{H}}$. When the decorrelating transformation $\boldsymbol{s} = \sqrt{2}\boldsymbol{\Xi}_{\mathrm{sq}}\boldsymbol{z} + \boldsymbol{\mu}$ is used, s_u is given by (14), and $\boldsymbol{z} = (z_1, z_2, \cdots, z_U)^*$. Therefor, $f_\Lambda(\lambda)$ becomes

$$f_\Lambda(\lambda) = \int_{-\infty}^{\infty}\cdots\int_{-\infty}^{\infty}\frac{1}{\pi^{\frac{U}{2}}}\left(\sum_{u=1}^{U}10^{-\frac{s_u}{10}}f_{\lambda_u}\left(10^{-\frac{s_u}{10}}\lambda\right)\prod_{k=1,k\neq u}^{U}F_{\lambda_k} \times\left(10^{-\frac{s_k}{10}}\lambda\right)\right)\times \mathrm{e}^{-\boldsymbol{z}^{\mathrm{H}}\boldsymbol{z}}\mathrm{d}z_1\cdots\mathrm{d}z_U. \tag{38}$$

Finally, the expectation in (31) can be evaluated with the use of (38). After doing some simplification works, we can conclude the proof.

APPENDIX C
PROOF OF PROPOSITION 1

We start the proof from an assumption that, the effect of number one in the logarithm terms can be ignored, the transmission power P_{t} in (9) and (10) therefore can be separated from integrals. Thereafter, by using Gauss, Gauss-Hermite, and Gauss-Laguerre quadratures on all of the capacity expressions, we can reduce the computational complexity and process do simplification works, and then we can conclude the proof. It should be noted that, more accurate estimation can be obtained by increasing the quadrature orders.

APPENDIX D
PROOF OF PROPOSITION 2

Staring from (31), if all MTs experience the same shadowing, (31) can be rewritten as

$$C_{\text{s-c.c.}} = \frac{B}{2\pi}\int_0^{2\pi} \mathbb{E}\left\{\log_2\left(1+\frac{P_{\mathrm{t}}\|\boldsymbol{d}\|\Phi(\omega)}{N_0 B}10^{\frac{s}{10}}\Lambda\right)\right\}\mathrm{d}\omega, \quad (39)$$

where $\Lambda = \max_{u\in\mathcal{U}}\lambda_u$ and $\lambda_u = \hat{d}_u\sum_{m=1}^{M}|r_{u,m}|^2$. The capacity then can be mathematically derived using the similar proof approach addressed in **Theorem 2**. Thereafter, by the help of numerical integration and the assumption of ignoring one in logarithm term, we can conclude the proof.

REFERENCES

[1] M. Liu, J. Yang, and G. Gui, "DSF-NOMA: UAV-assisted emergency communication technology in a heterogeneous Internet of Things," *IEEE Internet Things J.*, vol. 6, no. 3, pp. 5508–5519, Jun. 2019. doi: 10.1109/JIOT.2019.2903165.

[2] F. Boccardi, R. W. Heath, A. Lozano, T. L. Marzetta, and P. Popovski, "Five disruptive technology directions for 5G," *IEEE Commun. Mag.*, vol. 52, no. 2, pp. 74–80, Feb. 2014.

[3] V. W. Wong, R. Schober, D. W. K. Ng, and L. Wang, *Key Technologies for 5G Wireless Systems*. Cambridge, U.K.: Cambridge Univ. Press, 2017.

[4] A. Asadi, Q. Wang, and V. Mancuso, "A survey on device-to-device communication in cellular networks," *IEEE Commun. Surveys Tuts.*, vol. 16, no. 4, pp. 1801–1819, 4th Quart., 2014.

[5] M. Condoluci, L. Militano, A. Orsino, J. Alonso-Zarate, and G. Araniti, "LTE-direct vs. WiFi-direct for machine-type communications over LTE-A systems," in *Proc. IEEE PIMRC*, Hong Kong, Aug./Sep. 2015, pp. 2298–2302.

[6] Y. Hayashi, I. Shubhi, and H. Murata, "User collaboration for interference cancellation on multi-user MIMO communication systems," in *Proc. IEEE VTC Fall*, Boston, MA, USA, Sep. 2015, pp. 1–5.

[7] M. N. Soorki, M. H. Manshaei, B. Maham, and H. Saidi, "On uplink virtual MIMO with device relaying cooperation enforcement in 5G networks," *IEEE Trans. Mobile Comput.*, vol. 17, no. 1, pp. 155–168, Jan. 2018.

[8] *Study on Architecture Enhancements to Support Proximity Services (ProSe), Version 12.0.0*, document 3GPP TR 23.703, 2014.

[9] W. R. Heinzelman, A. Chandrakasan, and H. Balakrishnan, "Energy-efficient communication protocol for wireless microsensor networks," in *Proc. 33rd Annu. Hawaii Int. Conf. Syst. Sci.*, vol. 8, Jan. 2000, p. 10.

[10] Y. Li, L. Ding, and F. Liu, "The improvement of LEACH protocol in WSN," in *Proc. ICCSNT*, Dec. 2011, pp. 1345–1348.

[11] Y. Wu, J. C. Chen, L. P. Qian, J. W. Huang, and X. M. S. Shen, "Energy-aware cooperative traffic offloading via device-to-device cooperations: An analytical approach," *IEEE Trans. Mobile Comput.*, vol. 16, no. 1, pp. 97–114, Jan. 2017.

[12] R. Bordón, S. M. Sánchez, S. B. Mafra, R. D. Souza, J. L. Rebelatto, and E. M. G. Fernandez, "Energy efficient power allocation schemes for a two-user network-coded cooperative cognitive radio network," *IEEE Trans. Signal Process.*, vol. 64, no. 7, pp. 1654–1667, Apr. 2016.

[13] M. Costa and A. Ephremides, "Energy efficiency versus performance in cognitive wireless networks," *IEEE J. Sel. Areas Commun.*, vol. 34, no. 5, pp. 1336–1347, May 2016.

[14] R. Jayadi and Y.-C. Lai, "User cooperation in a multi-hop network with multi-interface devices for energy efficiency," in *Proc. IEEE Asia Pacific Conf. Wireless Mobile (APWiMob)*, Bandung, Indonesia, Sep. 2016, pp. 92–98.

[15] O. Zhao, L. Shan, W.-S. Liao, M. G. Kibria, H.-B. Li, K. Ishizu, and F. Kojima, "A device-centric clustering approach for large-scale distributed antenna systems using user cooperation," *IEICE Trans. Commun.*, vol. E102-B, no. 2, pp. 359–372, Feb. 2019.

[16] M. G. Kibria, K. Nguyen, G. P. Villardi, O. Zhao, K. Ishizu, and F. Kojima, "Big data analytics, machine learning, and artificial intelligence in next-generation wireless networks," *IEEE Access*, vol. 6, pp. 32328–32338, May 2018.

[17] H. Huang, S. Guo, G. Gui, Z. Yang, J. Zhang, H. Sari, and F. Adachi, "Deep learning for physical-layer 5G wireless techniques: Opportunities, challenges and solutions,", *IEEE Wireless Commun. Mag.*, to be published.

[18] Y. Wang, M. Liu, J. Yang, and G. Gui, "Data-driven deep learning for automatic modulation recognition in cognitive radios," *IEEE Trans. Veh. Technol.*, vol. 68, no. 4, pp. 4074–4077, 2019. doi: 10.1109/TVT.2019.2900460.

[19] H. Huang, Y. Song, J. Yang, G. Gui, and F. Adachi, "Deep-learning-based millimeter-wave massive MIMO for hybrid precoding," *IEEE Trans. Veh. Technol.*, vol. 68, no. 3, pp. 3027–3032, Mar. 2019.

[20] L. Ruan, M. P. I. Dias, and E. Wong, "Machine learning-based bandwidth prediction for low-latency H2M applications," *IEEE Internet Things J.*, vol. 6, no. 2, pp. 3743–3752, Apr. 2019.

[21] B. Hamdaoui, P. Venkatraman, and M. Guizani, "Opportunistic exploitation of bandwidth resources through reinforcement learning," in *Proc. IEEE GLOBECOM*, Honolulu, HI, USA, Nov./Dec. 2009, pp. 1–6.

[22] C. Xiao, J. Wu, S.-Y. Leong, Y. R. Zheng, and K. B. Letaief, "A discrete-time model for triply selective MIMO Rayleigh fading channels," *IEEE Trans. Wireless Commun.*, vol. 3, no. 5, pp. 1678–1688, Sep. 2004.

[23] O. Zhao and H. Murata, "Sum-rate analysis for centralized and distributed antenna systems with spatial correlation and inter-cell interference," *IEICE Trans. Commun.*, vol. E98-B, no. 3, pp. 449–455, Mar. 2015.

[24] O. Zhao and H. Murata, "A study on dynamic clustering for large-scale multi-user MIMO distributed antenna systems with spatial correlation," *IEICE Trans. Commun.*, vol. E99-B, no. 4, pp. 928–938, Apr. 2016.

[25] R. M. Gray, "On the asymptotic eigenvalue distribution of Toeplitz matrices," *IEEE Trans. Inf. Theory*, vol. IT-18, no. 6, pp. 725–730, Nov. 1972.

[26] C. Xiao and Y. R. Zheng, "On the Ergodic capacity of MIMO triply selective Rayleigh fading channels," *IEEE Trans. Wireless Commun.*, vol. 7, no. 6, pp. 2272–2279, Jun. 2008.

[27] M. Abramowitz and I. A. Stegun, *Handbook of Mathematical Functions: With Formulas, Graphs, and Mathematical Tables*, 9th ed. Washington, DC, USA: United States of America Department of Commerce, 1972.

[28] M. Lauridsen, L. Noël, T. B. Sørensen, and P. Mogensen, "An empirical LTE smartphone power model with a view to energy efficiency evolution," *Intel Technol. J.*, vol. 18, no. 1, pp. 172–193, Mar. 2014.

LIN SHAN received the M.E. and Ph.D. degrees from the Graduate School of Informatics, Kyoto University, in 2008 and 2012, respectively. From 2007 to 2008, he received the Merit Scholarship Program from the Ministry of Education, Recreation and Sports, Quebec, and was a Visiting Researcher with INRS-EMT, Quebec University, Canada. He is a Researcher with the National Institute of Information and Communications Technology (NICT), Japan. His research interests include network coding, multiuser-MIMO scheduling, cooperative relaying, and resource allocation in ad hoc and cellular networks. He received the Kyoto University President Prize, in 2010, the IEICE RCS Active Research Award, the IEEE VTS Japan Young Researcher's Encouragement Award, in 2011, the IEEE Kansai Section Student Paper Award, in 2012, and the IEICE Best Paper Award, in 2013.

OU ZHAO received the B.E. degree in electronics and communication engineering from the Nanjing University of Posts and Telecommunications (NJUPT), China, in 2005, and the M.E. and Ph.D. degrees in electronic engineering from the Graduate School of Informatics, Kyoto University, Kyoto, Japan, in 2014 and 2016, respectively. He is currently a Researcher with the Wireless Networks Research Center, National Institute of Information and Communications Technology (NICT). His major research interests include resource allocation, wireless signal processing, and its hardware implementation, machine learning, and big data analytics. He received the Young Researcher's Encouragement Award from the Japan Chapter of the IEEE Vehicular Technology Society (VTS), in 2013.

KATSUHIRO TEMMA received the B.E., M.E., and Ph.D. degrees in communications engineering from Tohoku University, Sendai, Japan, in 2010, 2012, and 2016, respectively. From 2013 to 2015, he was a Japan Society for the Promotion of Science (JSPS) Research Fellow. Since 2016, he has been with the National Institute of Information and Communications Technology (NICT). He is a member of the IEEE and the Institute of Electronics, Information and Communication Engineers (IEICE). He was a recipient of the IEEE VTS Japan Chapter 2011 Young Researcher's Encouragement Award.

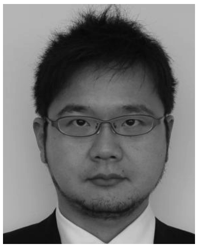

KIYOHIKO HATTORI received the M.E. degree from the University of Electro-Communications, in 2000, and the Ph.D. degree from the Tokyo Institute of Technology, in 2006. He is currently an Associate Professor with the Saitama Institute of Technology, Japan. His research interests include network systems, swarm robotics, and autonomous distributed systems.

FUMIHIDE KOJIMA received the B.E., M.E., and D.E. degrees in electrical and communications engineering from Osaka University, Osaka, Japan, in 1996, 1997, and 1999, respectively. He is currently the Director of the Wireless Systems Laboratory, Wireless Networks Research Center, National Institute of Information and Communications Technology, Yokosuka, Japan. Since he joined the Communications Research Laboratory, Ministry of Posts and Telecommunications, in 1999, he has been involved in research on various topics, such as intelligent transportation systems, radio-over-fiber multimedia transmissions, mobile ad hoc emergency networks, wireless grid systems, and medium access control protocol for communications systems. He is a member of the IEEE.

FUMIYUKI ADACHI received the B.S. and Dr.Eng. degrees in electrical engineering from Tohoku University, Sendai, Japan, in 1973 and 1984, respectively. In 1973, he joined Electrical Communications Laboratories, Nippon Telegraph and Telephone Corporation (now NTT), and conducted research on digital cellular mobile communications. From 1992 to 1999, he was with NTT DOCOMO, where he led a research group on wideband/broadband wireless access for 3G and beyond. He contributed to the development of 3G air interface standard, known as W-CDMA. Since 2000, he has been with Tohoku University. He was a Full Professor with the Department of Communications Engineering, Graduate School of Engineering, until 2016. From 1984 to 1985, he was a United Kingdom SERC Visiting Research Fellow with the Department of Electrical Engineering and Electronics, Liverpool University. He is currently a Specially Appointed Professor for Research with the Research Organization of Electrical Communication (ROEC), Tohoku University, and is leading a wireless signal processing research group aiming at 5G systems and beyond. His research interests include the area of wireless signal processing and networking, including multi-access, equalization, antenna diversity, adaptive transmission, channel coding, and radio resource management.

Dr. Adachi is an IEEE Life Fellow and an IEICE Fellow and has been an IEEE VTS Distinguished Lecturer/Speaker, since 2011. He was a recipient of the IEEE Vehicular Technology Transactions Best Paper of the Year Award, in 1980 and 1990, the IEICE Transactions Best Paper of the Year Award, in 1996, 1998, and again in 2009, the IEEE VTS Avant Garde Award, in 2000, the IEICE Achievement Award, in 2002, the IEEE VTS Conference Chair Award, in 2014, the IEEE VTS Conference Chair Award, in 2014, the IEEE VTS Stuart Meyer Memorial Award, in 2017, the IEEE ComSoc RCC Technical Recognition Award, in 2017, the Thomson Scientific Research Front Award, in 2004, the Ericsson Telecommunications Award, in 2008, the Telecom System Technology Award, in 2009, the Prime Minister Invention Prize, in 2010, the British Royal Academy of Engineering Distinguished Visiting Fellowship, in 2011, the KDDI Foundation Research Award, in 2012, the C&C Prize, in 2014, the Rinzaburo Shida Award, in 2016, the Sendai Municipal Commendation, in 2017, the IEEE VTS Stuart Meyer Memorial Award, in 2017, and the IEEE ComSoc RCC Technical Recognition Award, in 2017. He is listed in Highly Cited Researchers, in 2001 (http://hcr.stateofinnovation.thomsonreuters.com/page/archives).